

Correlations in magnitude series to assess nonlinearities: application to multifractal models and heartbeat fluctuations

Pedro A. Bernaola-Galván¹, Manuel Gómez-Extremera¹, A. Ramón Romance² and Pedro Carpén¹

¹ Dpto. de Física Aplicada II. ETSI de Telecomunicación. University of Málaga. 29071 Málaga, Spain

² Dpto. de Didáctica de la Lenguas, las Artes y el Deporte. Facultad de C.C. E.E. University of Málaga. 29071 Málaga, Spain.

The correlation properties of the magnitudes of a time series (sometimes called volatility) are associated with nonlinear and multifractal properties and have been applied in a great variety of fields. Here, we have obtained analytically the expression of the autocorrelation of the magnitude series of a linear Gaussian noise as a function of its correlation as well as several analytical relations involving them. For both, models and natural signals, the deviation from these equations can be used as an index of non-linearity that can be applied to relatively short records and that does not require the presence of scaling in the time series under study. We apply this approach to show that the heart-beat records during rest show higher non-linearities than the records of the same subject during moderate exercise. This behavior is also achieved on average for the analyzed set of 10 semiprofessional soccer players. This result agrees with the fact that other measures of complexity are dramatically reduced during exercise and can shed light on its relationship with the withdrawal of parasympathetic tone and/or the activation of sympathetic activity during physical activity.

PACS numbers: 05.40.- a, 05.45.Tp

I. INTRODUCTION

Since the pioneering works [1], much attention has been paid to the study of correlations in time series of interbeat intervals (*RR* time series), in fact it has been revealed as a powerful tool to evaluate alterations due to disease or aging [2, 3], discriminate between physiological states [4] and assess the state of fitness [5, 6]. In most cases, studies are limited to linear correlations (power-spectrum, auto-correlation function, DFA, etc.) but non-linear correlations are indeed present in *RR* time series [7] and are supposed to play an important role in heart dynamics as their reduction or absence has been related to aging and certain pathological conditions [8, 9].

In the field of time series analysis, the concept of non-linearity can be interpreted in different ways [10]. According to the definition of Schreiber and Schmitz [11] a time series is linear when its Fourier phases are random. Based on this definition, the presence of non-linear correlations in a time series can be assessed by means of surrogate data tests: (i) The random phases of the signal are randomized preserving their linear correlations (power-spectrum) and the distribution of data [11] (ii) Some relevant statistics is evaluated in the original as well as in the surrogated signal and, if there is a statistically significant difference, the null hypothesis of linearity can be rejected. Sometimes instead of accepting or rejecting the null hypothesis, the goal is simply to compare the degree of non-linearity of two different time series (e.g. records obtained under different physiological conditions) and the value of the statistics is directly used as a measure of non-linearity.

The autocorrelations in the magnitude series is a good indicative of the presence of non-linear correlations.

Given a time series $\{y_i\}$, its magnitude series (sometimes also called volatility) is usually defined as the absolute value of the series increments:

$$|x_i| = |y_{i+1} - y_i|. \quad (1)$$

One of the quantities used to measure the non-linearity in heart rate series is the scaling exponent of its magnitude series, calculated by means of the Detrended Fluctuation Analysis (DFA) [9]. In brief, the DFA method obtains the squared mean quadratic fluctuations of the series around the local trend $F_d(\ell)$ in all windows of a given size ℓ and repeat the procedure for different window sizes. Scaling is present when

$$F_d(\ell) \propto \ell^\alpha. \quad (2)$$

Typically, α is estimated as the slope of a linear fitting of $\log(F_d)$ vs. $\log(\ell)$. The exponent α quantifies the strength of the correlations present in the time series and is also related to the power spectrum exponent β and the autocorrelation function exponent γ [12, 13].

Examples of the study of non-linearity using the DFA exponent of the magnitude series can be found not only in heart rate analysis but also in many other fields as Fluid Dynamics [14], Geophysical [10, 15, 16] and Economical time series [17]. This quantity is easy to compute and is also related to the width of the multifractal spectrum [18, 19], another quantity also frequently used to unveil the non-linear properties of a signal.

Nevertheless, this approach shows three main drawbacks:

- (i) In order to properly define the scaling exponent α , $F_d(\ell)$ vs. ℓ must show a good fit to a power-law, which is not the case in many natural series. Also,

the interpretation of crossovers in $F_d(\ell)$ vs. ℓ as a signature of the existence of regions with different scaling has been recently challenged. In particular, it has been shown that the evaluation of short-range scaling exponent (α_1), a quantity widely used in heart rate analysis [20], could be affected by spurious results [21] and that α_1 is strongly biased by the breathing frequency [22]. Without judging the validity of these criticisms, the truth is that some results obtained with α_1 are contradictory [23]. These problems affect to DFA in general as a technique for evaluating scaling exponents.

- (ii) Furthermore, particularizing to the evaluation of the scaling exponent of the magnitude series, we have shown very recently that in some situations DFA does not properly detect the correlations and assigns uncorrelated behavior to correlated magnitude series [24].
- (iii) It is assumed implicitly that the presence of correlations in the magnitude series is a signature of non-linearity but, as we show later, even for a linear time series the autocorrelation of the magnitude series can be different from zero.

For these reasons we propose here a different approach. We obtain analytically the expression of the autocorrelation function of the magnitude series as a function of the autocorrelation function of the original series for a linear Gaussian noise and propose the deviation from this equation as a good signature of non-linear correlations. Taking into account that natural data does not always follow Gaussian distributions, prior to the computation of the magnitude correlations, we transform the distribution of the data to a $\mathcal{N}(0, 1)$.

This article is organized as follows: In section II we obtain the analytical expression of the autocorrelation of magnitude series of a linear Gaussian noise as a function of the autocorrelation of the original series as well as a quadratic approximation. We also obtain the corresponding expression for the square series which is sometimes used to study the non-linear correlations (Sec. II A) and discuss about the autocorrelation of the sign series and its relation to the autocorrelation of the magnitude series (Sec. II B). In section III we explore the non-linear properties of artificial series generated with a model that produces Gaussian noises with multifractal properties and in section IV, as an example of their utility, we apply the relations derived here to the study of heart beat time series during rest and moderate exercise. Section V concludes the paper.

II. AUTOCORRELATION OF MAGNITUDE SERIES

Given a time series $\{y_i\}$, with its corresponding series of increments $\{x_i\}$, our aim is to obtain the autocorrelation

of its magnitude series $\{|x_i|\}$, $C_{|x|}(\ell)$ as a function of the autocorrelation of the series of increments $C_x(\ell)$ provided that $\{x_i\}$ is linear gaussian noise, i.e. all $x_i \sim \mathcal{N}(0, 1)$ (normally distributed with zero mean and unit standard deviation) and that only linear correlations are present in the series. Thus, the autocorrelation function $\{x_i\}$ at distance ℓ is given by:

$$C_x(\ell) = \frac{\langle x_i \cdot x_{i+\ell} \rangle - \langle x_i \rangle \langle x_{i+\ell} \rangle}{\sigma_x^2} = \langle x_i \cdot x_{i+\ell} \rangle, \quad (3)$$

where $\langle \cdot \rangle$ denotes average over the series and σ_x^2 is the variance of the series.

Under this assumption the autocorrelation coincides with the autocovariance

$$K_x(\ell) \equiv \langle x_i \cdot x_{i+\ell} \rangle - \langle x_i \rangle \langle x_{i+\ell} \rangle = C_x(\ell). \quad (4)$$

On the other hand, for the magnitude series we have:

$$\sigma_{|x|}^2 = 1 - \frac{2}{\pi}, \quad (5)$$

and we can write for its autocorrelation:

$$\begin{aligned} C_{|x|}(\ell) &= \frac{\langle |x_i| \cdot |x_{i+\ell}| \rangle - \langle |x_i| \rangle \langle |x_{i+\ell}| \rangle}{\sigma_{|x|}^2} \\ &= \frac{\pi K_{|x|}(\ell)}{\pi - 2}, \end{aligned} \quad (6)$$

Taking into account that X_i and $X_{i+\ell}$ are two linearly correlated Gaussian random variables, the autocovariance of the magnitude series, $K_{|x|}(\ell)$, can be expressed as a function of $K_x(\ell)$ according to Eq. (A12) in appendix A:

$$K_{|x|} = \frac{2}{\pi} \left[\sqrt{1 - K_x^2} + K_x \arcsin K_x - 1 \right], \quad (7)$$

and replacing in (6):

$$C_{|x|} = \frac{2 \left[C_x \arcsin C_x - 1 + \sqrt{1 - C_x^2} \right]}{\pi - 2} \quad (8)$$

It is easy to check that (8) is always positive which implies that the magnitude of a linear Gaussian noise cannot be anticorrelated (Fig. 1).

If we consider small values of the autocorrelation we can approximate (8) by Taylor expansion and obtain:

$$C_{|x|} = \frac{1}{\pi - 2} C_x^2 + \mathcal{O}(C_x^4) \quad (9)$$

Thus, for small values, the autocorrelation of the magnitude series behaves essentially as the square of the autocorrelation of the original series. In fact, the error of (9) is around 2% for $C_x = 0.5$ which make this approximation virtually correct for most real data. In figure 1 we plot Eq. (8), its quadratic approximation Eq. (9) as

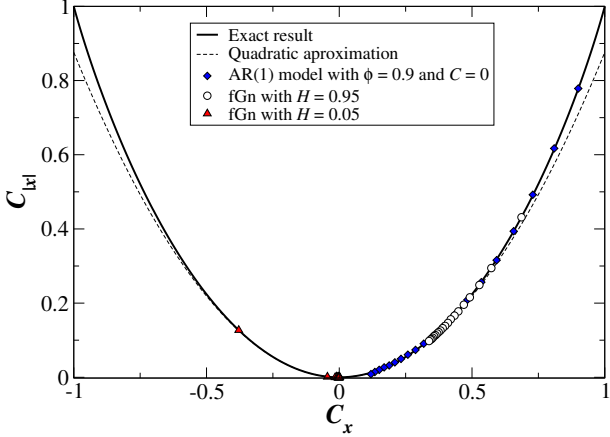


FIG. 1. (Color online) Autocorrelation of the magnitude series $C_{|x|}$ as a function of the autocorrelation of the original series C_x . Solid line correspond to the exact expression given by Eq. (8) and dashed line to its quadratic approximation given by Eq. (9). The symbols correspond to the autocorrelation at distances $\ell = 1, \dots, 20$ for several artificial series generated with linear Gaussian models: diamonds, autoregressive AR(1) model $x_i = c + \phi x_{i-1} + \varepsilon_i$, with $\phi = 0.9$, $c = 0$ and $\{\varepsilon_i\}$ a white noise; circles, fractional Gaussian noise (fGn) with power spectrum exponent $H = 0.95$ and triangles fGn with $H = 0.05$. While the two first models (diamonds and circles) generate highly correlated series the last one (triangles) leads to an anticorrelated series. However, in all cases the correlations of the magnitude series are positive.

well as several examples of artificial series created with Gaussian linear models.

This result is especially interesting when studying the scaling behavior of series with power-law correlations that have been found in a great variety of complex systems. We can characterize these series by their power spectral exponent β because most methods of generating power-law correlated Gaussian noises consist in the generation of series with $1/f^\beta$ decay in their power spectrum with $-1 < \beta < 1$ (e.g. [25, 26]). In particular, these methods are widely used to generate approximate fractional Gaussian noises (fGn). The autocorrelation function of these models asymptotically verifies [27]:

$$C_x(\ell) \simeq \frac{(1-\gamma)(2-\gamma)}{2\ell^\gamma} \propto \frac{\text{sgn}(1-\gamma)}{\ell^\gamma} \quad (10)$$

where $\gamma = 1 - \beta$. It is also quite common to characterize the fGns by their Hurst exponent (H) which is related to both β and γ by:

$$H = \frac{\beta + 1}{2} = \frac{2 - \gamma}{2} \quad (11)$$

For stationary time series ($H < 1$), the Hurst exponent also coincides with the DFA exponent α . Note that the term $\text{sgn}(1-\gamma)$ in the numerator of (10) vanishes for $\beta = 0, H = 0.5$ (white noise) thus leading to an uncorrelated random noise. For $\beta > 0, H > 0.5$ the series is

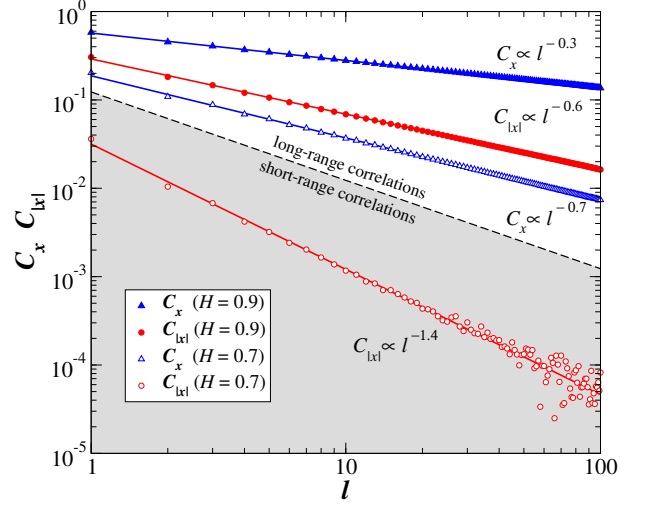


FIG. 2. (Color online) Autocorrelation function C_x (triangles) and autocorrelation function of magnitude series $C_{|x|}$ (circles) as a function of distance ℓ for two examples of fractional Gaussian noises (fGn): $H = 0.9 > 0.75$ (full symbols) and $H = 0.7 < 0.75$ (open symbols). We generate series of approximate fGns of length $2^{24} \simeq 1.6 \times 10^7$ using the Fourier Filtering Method [26]. To avoid statistical fluctuations we average over an ensemble of 100 realizations. The dashed line correspond to $1/\ell$ which is the boundary between the regions of long and short-range correlations (see text). As expected, $C_{|x|}$ decays with an exponent double that of C_x and in both cases the magnitude series are positively correlated but for $H = 0.7 < 0.75$, $C_{|x|}$ decays faster than $1/\ell$ and lies in the short-range correlations region. Note also that in this case and due to both the fast decay of $C_{|x|}$ and its small values at $\ell = 1$, a noisy behavior is reached relatively soon ($\ell < 100$) even for long series. This makes difficult the detection of power-law behaviors in this region when dealing with real data.

long-range correlated, also known as having “long memory” [13, 27], in the sense that its autocorrelation decays very slow with exponent $\gamma < 1$. In fact $\sum_{\ell=1}^L C_x(\ell)$ diverges as $L \rightarrow \infty$. Likewise for $\beta < 0, H < 0.5$, i.e. $\gamma > 1$, C_x is negative and the series is anticorrelated. In this situation, although the autocorrelation also decays as a power law, we cannot properly speak about long-range anticorrelations because they decay relatively fast, in the sense that now the autocorrelation function is summable. Another conclusion drawn from (10) is that we cannot obtain linear Gaussian noises with positive autocorrelation functions decaying faster than $1/\ell$.

We also obtain from (9) that the autocorrelation of the magnitude series of a fGn also decays as a power law with exponent 2γ and is always positive, even for $H < 0.5$ when the original series is anticorrelated:

$$C_{|x|} \propto \frac{1}{\ell^{2\gamma}} \quad (12)$$

Nevertheless, we must distinguish two different situations:

(i) $H > 0.75$. Here $2\gamma < 1$ and $C_{|x|}$ decays slower

than $1/\ell$ thus leading to long-range power-law correlations in the magnitude series.

(ii) $H < 0.75$. Now $2\gamma > 1$ and $C_{|x|}$, although still being positive and following a power-law, decays very fast. For example, in Fig. 2 we can see that for $H = 0.7$, $C_{|x|}$ reaches the background noise level for relatively short scales ($\ell < 100$) even for a time series as long as $2^{24} \simeq 1.6 \times 10^7$.

Indeed, the methods quantifying correlations by means of the study of fluctuations fail to detect the power-law correlations present in magnitude series for $H < 0.75$. For example, two widely used techniques like Fluctuation Analysis (FA) or Detrended Fluctuation Analysis (DFA) [28] wrongly classify as “white noise” the magnitude series of Gaussian noises with $H < 0.75$ [18, 19] despite being true only for $H = 0.5$ [24].

A. Relation with the autocorrelation of square series

For simplicity, sometimes the autocorrelation of square series is studied instead of the magnitude series, i.e.:

$$C_{x^2}(\ell) = \frac{\langle x_i^2 \cdot x_{i+\ell}^2 \rangle - \langle x_i^2 \rangle \langle x_{i+\ell}^2 \rangle}{\sigma_{x^2}^2} \quad (13)$$

Indeed, it has been shown numerically that the scaling properties of the correlations of both series are quite similar [18]. Below we justify analytically this similarity.

As we did for the magnitude series, first we obtain the autocovariance of the square series, K_{x^2} , as a function of the autocovariance of the original series, K_x (Appendix B):

$$K_{x^2}(\ell) \equiv \langle x_i^2 \cdot x_{i+\ell}^2 \rangle - \langle x_i^2 \rangle \langle x_{i+\ell}^2 \rangle = 2K_x(\ell)^2, \quad (14)$$

and taking into account that $\sigma_{x^2} = \sqrt{2}$ we obtain:

$$C_{x^2} = C_x^2 \quad (15)$$

Which obviously implies that the autocorrelation of the squares of a linear Gaussian noise, just as the magnitude, cannot be anticorrelated.

Eq. (15) also justifies the fact that for power-law correlated series, $C_{|x|}$ and C_{x^2} scale asymptotically with the same exponent: for long enough values of ℓ we have $C_x \ll 1$ and thus the approximation (9) is valid, leading to $C_{|x|} \propto C_{x^2}$.

B. Relation with the autocorrelation of the sign series

Apart from its relevance in the study of non-linear correlations, the magnitude series together with the sign series (defined below) provide complementary information

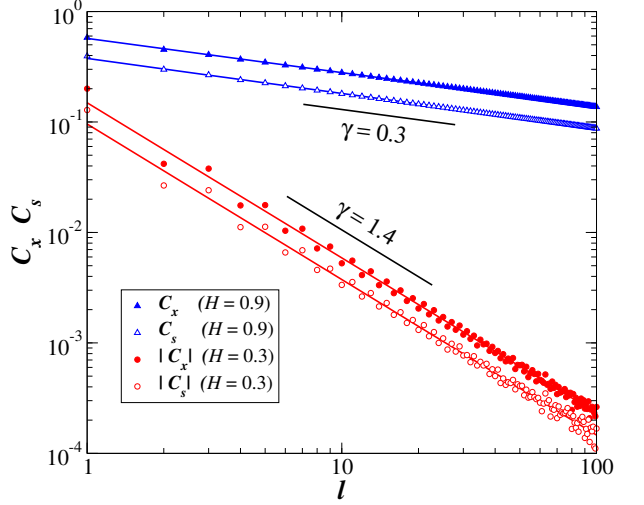


FIG. 3. (Color online) Autocorrelation function C_x (full symbols) and autocorrelation function of sign series C_s (open symbols) as a function of distance ℓ for two examples of fractional Gaussian noises (fGn): correlated $H = 0.9 > 0.5$ (triangles) and anticorrelated $H = 0.3 < 0.5$ (circles). In this case we plot $|C_x|$ and $|C_s|$ to allow the representation in double logarithmic scale. We generate series of approximate fGns of length $2^{24} \simeq 1.6 \times 10^7$ using the Fourier Filtering Method [26]. To avoid statistical fluctuations we average over an ensemble of 100 realizations. As can be expected from (18), C_x and C_s decay with the same exponent. Note that for the anticorrelated series ($H = 0.3$) the anticorrelations decay very fast ($\gamma = 1.4$) and an oscillatory behavior can be observed. This oscillation is amplified for $H < 0$ (not shown).

about the original series: while the magnitude measures how big the changes are, the sign indicates their direction. Sign series are also relevant for the study of first-passage time in correlated processes [29]. Below we obtain a relation between the $C_{|x|}$ and the autocorrelation of the sign series C_s . Given a time series $\{x_i\}$, the series $\{\text{sgn}(x_i)\}$ defined by:

$$\text{sgn}(x) = \begin{cases} -1 & \text{if } x < 0 \\ 0 & \text{if } x = 0 \\ 1 & \text{if } x > 0 \end{cases} \quad (16)$$

If the original series $\{x_i\}$ is a linear Gaussian noise, Apostolov et al. [30] have shown that the autocorrelation of the sign series $C_s(\ell)$ can be expressed in terms of the correlation of the series $C_x(\ell)$ by:

$$C_s = \sin\left(\frac{\pi}{2}C_x\right) \quad (17)$$

Again, we can also obtain an approximation for small values of $C_x(\ell)$:

$$C_s = \frac{2}{\pi}C_x + \mathcal{O}(C_x^3) \quad (18)$$

which implies that the autocorrelation of the sign series scales asymptotically with the same exponent as the correlation of the original series.

In addition and, taking into account that $-1 \leq C_s \leq 1$, from here it is clear that C_x and C_s always have the same sign and thus, the sign series will be correlated where original series is correlated and anticorrelated where the original series is anticorrelated (Fig. 3).

Equation (17), together with (8) allows us to express the autocorrelation of the magnitude series as a function of the autocorrelation of the corresponding sign series:

$$C_{|x|} = \frac{2}{\pi - 2} \left[\frac{\pi}{2} C_s \sin \left(\frac{\pi}{2} C_s \right) + \cos \left(\frac{\pi}{2} C_s \right) - 1 \right] \quad (19)$$

III. EXAMPLE OF A NONLINEAR MODEL

Up to now we have only shown examples of linear Gaussian signals for which the derived relations among C_x , $C_{|x|}$ and C_s (Eqs. (8), (17) and (19)) must hold. Nevertheless, for nonlinear Gaussian signals these relations are no longer valid and the deviation from these equations can be used as a signature of nonlinearity. Here it is important to stress that these equations are valid for each individual value of the autocorrelation function and the possible deviations from nonlinearity can be observed without the assumption of any kind of scaling or power-law behavior in the signal.

We concentrate here on equation (8) because the correlations in the series of magnitudes have been related to the presence of nonlinear correlations and multifractal structure [9, 18, 19]. To show the effect of nonlinearities we generate artificial series using a simple method proposed by Kalisky et al. [18] which is able to generate multifractal Gaussian noises just by multiplying the sign and the magnitude of two independent linear Gaussian noise. Despite its simplicity, this method is able to independently control both the linear correlations of the signal and its multifractal spectrum width — see also [19] for a systematic exploration of the method.

In brief this procedure, *composition method* from now on, works as follows:

- Obtain the magnitude series of a fGn $\{x_{\text{mag}}(i)\}$, with Hurst exponent H_1 and the sign series of another fGn $\{x_{\text{sign}}(i)\}$, with Hurst exponent H_2 , where $i = 1, \dots, N$, being N the size of the series.
- Obtain the composed series as the product of the magnitude and sign series:

$$x_{\text{comp}}(i) = x_{\text{mod}}(i) \cdot x_{\text{sign}}(i) \quad (20)$$

for $i = 1, \dots, N$.

The resulting series is Gaussian by construction but it has nonlinear correlations and Eq. (8) is not fulfilled. Instead, it can be shown that its autocorrelation function is given by [19]:

$$C_x(\ell) = C_s(\ell) \frac{(\pi - 2)C_{|x|}(\ell) + 2}{\pi} \quad (21)$$

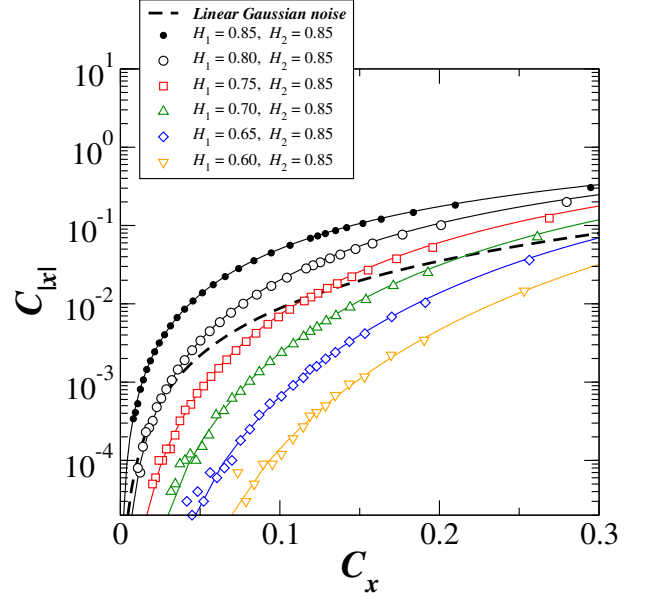


FIG. 4. (Color online) Autocorrelation of the magnitude series $C_{|x|}$ as a function of the autocorrelation of the original series C_x for nonlinear series generated using the *composition method* [19] by multiplying the series of magnitudes and signs of two independent fGns (see text). Eq. (8) (dashed line) has been included as a reference for the linear Gaussian noise. Solid lines correspond to the theoretical curves obtained using (21) and assuming that the fGns verify the exact asymptotic formula for their autocorrelation function (10). Eq. (21) is exact, the observed deviations from these curves are due to the fact that the series generated by means of the Fourier filtering method are approximate fGns, the expression used for the autocorrelation are valid only asymptotically and also to due to the statistical fluctuations (especially for small values of $C_{|x|}$).

where obviously $C_{|x|}$ and C_s coincide with the autocorrelation functions of the magnitude of the fGn with H_1 and the sign of the fGn with H_2 respectively. Note that, although C_x is not exactly a power law, it decays asymptotically as $1/\ell^{2-2H_2}$, i.e. the autocorrelation of the composed series decays asymptotically with the same exponent as the autocorrelation of the fGn used to obtain the sign series. Indeed, just take into account approximations (9) for $C_{|x|}$ and (18) for C_s and the asymptotic expression for the autocorrelation of a fGn (10) to obtain:

$$C_x(\ell) \simeq \frac{2H_2(2H_2 - 1)}{\pi^2 \ell^{2-2H_2}} \left[\frac{H_1^2(2H_1 - 1)^2}{\ell^{4-4H_1}} + 2 \right]. \quad (22)$$

For $H_1, H_2 < 1$ the second term is the leading one and we get asymptotically $C_x(\ell) \propto 1/\ell^{2-2H_2}$. In that sense we say that the linear correlations of the composed series are *controlled* by the sign [19].

In Fig. 4 we show $C_{|x|}$ vs. C_x for several examples of nonlinear series generated by means of the composition method. For all the series shown $H_2 = 0.85$ and thus, all of them have the same scaling behavior for the linear correlations, nevertheless the different values of H_1 lead

to different degrees of nonlinearity according to the deviation of $C_{|x|}$ from the linear expectation (dashed line in Fig. 4). Note that, no matter the value of H_1 , in all cases we observe a deviation from linearity. For smaller values of H_1 this deviation is more evident at small C_x (longer scales) while for large H_1 it appears mainly at great C_x (small scales).

This means that the uncoupling of magnitude and sign (i.e. the magnitude of the changes is independent of its direction) always leads to a nonlinear behavior or, conversely, in a linear Gaussian signal magnitude and sign are not independent but coupled in a specific way that leads to the behavior described by Eq. (8). In general, for natural signals where magnitude and sign are not independent nor *Gaussianily coupled*, plots of $C_{|x|}$ vs. C_x can be of great utility to shed light about the way in which the magnitude of the changes is related to its direction, i.e. the magnitude and sign coupling.

A. Nonlinearity and multifractality

Multifractality and nonlinearity are two concepts that usually go together. Indeed, the width of the multifractal spectrum is considered to be linked to the degree of nonlinearity of the signal [31, 32] and the finding of multifractal properties is usually associated with complex nonlinear interactions in the systems under study. Nevertheless, although related concepts, multifractality and nonlinearity describe the properties of the signal from different points of view [33].

The nonlinear signals generated by means of the composition method described here are a good example to show that nonlinearity is not always related to multifractality. This method was originally developed [18] to generate Gaussian signals with multifractal properties, in fact, it has been shown that the width of the multifractal spectrum grows linearly with the hurst exponent H_1 of the signal used to obtain the magnitude series for $H_1 > 0.75$ and when $H_1 < 0.75$ the width of the multifractal spectrum almost vanishes [19]. Nevertheless, we show here (Fig. 4) that for all values of H_1 (including the white noise for which $H_1 = 0.5$) the composed signal is clearly nonlinear, despite having an almost zero multifractal spectrum width. Here, it is important to point out that the region where multifractal detrending techniques give null multifractal width ($H_1 < 0.75$) [19] coincide with the region where $C_{|x|}$ lies below the linear expectation, at least in the region where the power law fits are carried out ($\ell > 4$). According to this, we can say that, at least for this model, multifractality is a signature of non-linearity but only when the autocorrelations in the module larger than expected in a linear model. In the opposite situation, the time series is indeed non-linear but the multifractal analysis will not reveal it.

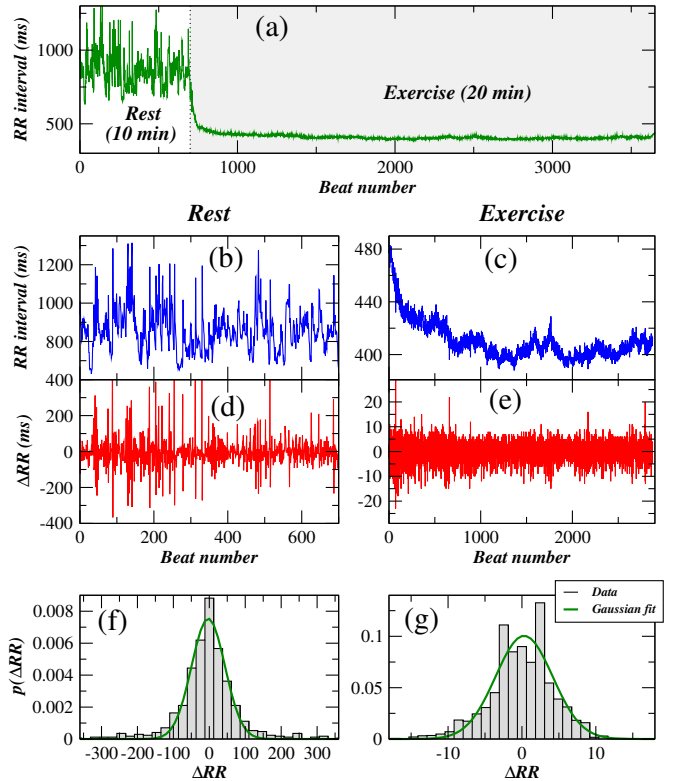


FIG. 5. (Color online) Record of interbeat intervals (RR) during rest and moderate exercise for a semi-professional soccer player. (a) Full record of 10 minutes resting in supine position on the soccer field plus 20 minutes running at moderate pace. (b)(c) Separate records for rest and exercise. (d) (e) Series of increments ΔRR for rest and exercise. (f)(g) Distributions of ΔRR . For comparison it has been included the best fit to a Gaussian distribution (thick line).

IV. EXAMPLE OF NATURAL SIGNALS: HEART RATE DURING REST AND EXERCISE

Regarding the heart rate during exercise, it is well known that heartbeat dynamics can change dramatically with physical activity. The most evident changes being the abrupt increase in the heart-rate (i.e. reduction of the mean RR intervals) and the reduction of the heart rate variability (HRV), i.e. the variance of the RR times series [34]. In addition to these features that can be observed by direct inspection of raw RR time series (Fig. 5.a), it has been also found that exercise modifies the distribution of the power spectrum by reducing the low frequency components [23, 34, 35] and introducing very high frequencies related to the respiration rate [36], decreases the sample entropy [37] and the linear correlations measured by the short scale DFA exponent (α_1), are not only reduced with exercise [37, 38] but also can be correlated with the intensity of the exercise [39]. Nevertheless it is fair to say that the opposite result can also be found in the literature [40]. In summary, despite this last contradiction, the general agreement is that in

a wide sense the complexity of the RR time series is reduced during exercise and that this effect is related to the breakdown of the equilibrium between the two branches of the autonomic nervous systems due to the withdrawal of parasympathetic tone and/or the activation of sympathetic activity (see [23, 36] for reviews).

Here we hypothesize that this reduction in complexity should also be reflected in the lost of nonlinearity in the heart dynamics during exercise. In particular, we concentrate ourselves on short scales because it has been reported that in this range ($\ell < 11$ beats) linear correlations seem to be clearly affected by the intensity of the exercise and because, in practice, the typical length of the records at rest is rarely longer than 10-15 minutes (500-1000 beats) to avoid excessive interferences with the training sessions, thus preventing from accurate evaluation of autocorrelation functions beyond at long distances.

We analyze records during rest and moderate exercise from 10 semi-professional soccer players all of them healthy males (age 23.8 ± 2.9 yr) without any prior history of cardiovascular disease. Each record includes two stages: (i) 10 minutes of normal wake rest condition, laying in supine position on the soccer field (ii) followed by 20 minutes of moderate running, i.e. at typical warming-up pace (Fig. 5.a). Heart rate was monitored beat-by-beat using a Polar S810i RR cardiotachometer (Polar Electro, Oy, Finland) [41].

As RR time series are typically non-stationary, especially during exercise (Figs. 5.b and c), it is a common practice to analyze the series of its increments (ΔRR) which are quite stationary, at least in weak-sense (Figs. 5.d and e). Following the notation introduced in Sec. II $\{y_i\}$ would be the series of RR intervals while $\{x_i\}$ would be the series of interbeat intervals increments (ΔRR).

The distributions of ΔRR are fairly symmetric, although they are not exactly Gaussian but Levy-stable distributions with tails decaying slower than in the Gaussian case [1] (Figs. 5.f and g). For this reason, prior to the analysis we convert the distribution of the data to a standard normal distribution by means of the transformation:

$$x' = \Phi^{-1}[F(x)] \quad (23)$$

where $F(\cdot)$ is the cumulative distribution of the original ΔRR data and $\Phi(\cdot)$ is the cumulative standard normal distribution $\mathcal{N}(0, 1)$. We have observed that this transformation practically does not affect to the linear correlations C_x (not shown).

For each subject we compute the autocorrelation function of the signal $C_x(\ell)$ and the magnitude series $C_{|x|}(\ell)$ for both rest and exercise records.

In Fig. 6 we show the results for one of the subjects for $\ell = 1, \dots, 20$. In general, we observe that C_x reaches similar values during rest and exercise or even greater values for the latter (Fig. 6.b) but, on the other hand, $C_{|x|}$ is typically greater during rest (Fig. 6.c). In addition, if we inspect carefully Fig. 6.a it is clear that not only

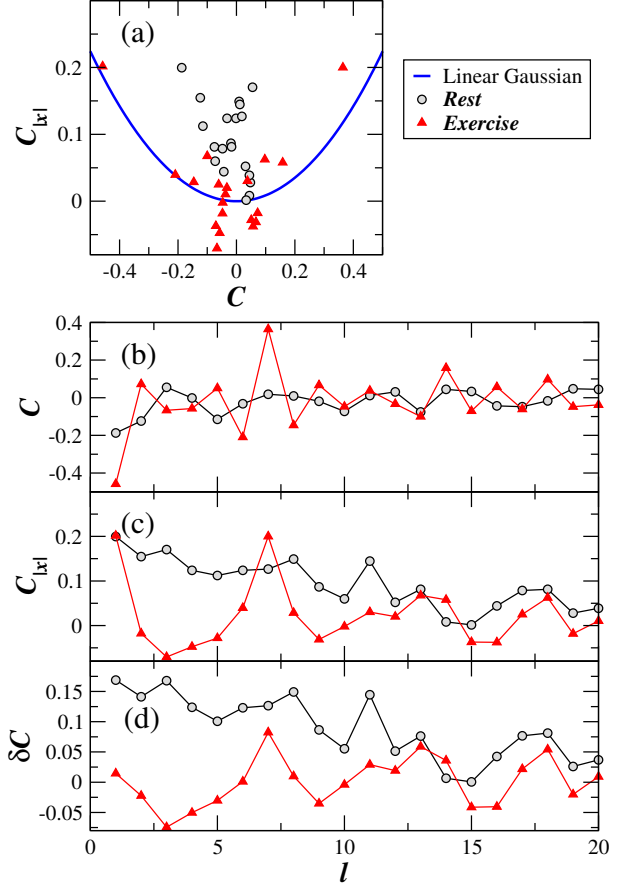


FIG. 6. (Color online) Autocorrelation C_x and autocorrelation of the magnitude $C_{|x|}$ for the series of increments ΔRR during rest and exercise shown in Fig. 5. (a) $C_{|x|}$ vs. C_x during rest (circles) and exercise (triangles). The thick line corresponds to the theoretical expectation for a linear Gaussian noise (8). (b) Autocorrelation $C_x(\ell)$ as a function of the lag ℓ during rest and exercise. (c) Autocorrelation of magnitude series $C_{|x|}(\ell)$ as a function of the lag ℓ during rest and exercise. (d) Difference between $C_{|x|}$ and the theoretical expectation for a linear Gaussian noise given C_x (see text) as a function of the lag ℓ during rest and exercise.

the values of $C_{|x|}$ are greater on average for rest than for exercise but also the exercise records are closer to the thick line (expectation for a Gaussian linear noise). For this reason a good measure of non-linearity is not simply the autocorrelation in the magnitude $C_{|x|}$ but its difference with the expectation for a linear Gaussian noise computed using using Eq. (8) (thick line in Fig. 6.a):

$$\delta C = C_{|x|} - C_{|x|, \text{teor}}(C_x) \quad (24)$$

This quantity takes into account not only the value of $C_{|x|}$ but also its difference with the linear expectation. For example $C_{|x|}(\ell = 1)$ reaches a relatively high value for both, rest and exercise (Fig. 6.c) but, once substracted the linear expectation $\delta C(\ell = 1)$ is much higher for rest than for exercise (Fig. 6.d).

In order to obtain a single number to quantify the

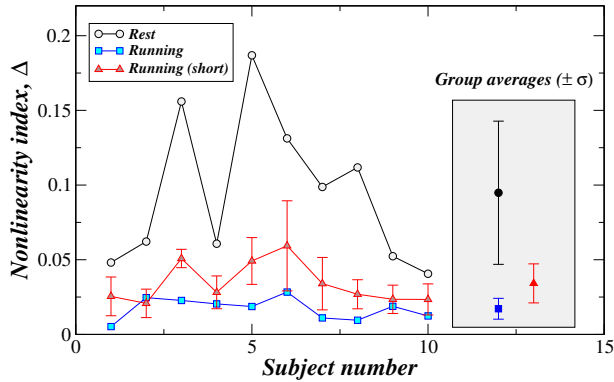


FIG. 7. (Color online) Nonlinearity index Δ ($\ell_{\max} = 10$) for 10 semiprofessional soccer players, all males with age 23.8 ± 2.9 yr. Circles: records of 10 minutes of normal wake rest condition, laying in supine position on the soccer field. Squares: 20 minutes of running at typical warming-up pace. Triangles: average of Δ over an ensemble of sub-series of the running record with the same size of the corresponding rest record (see text). Error bars indicate \pm standard deviation.

non-linearity of a signal we propose here the sum of the squares of the curve $\delta C(\ell)$:

$$\Delta = \sum_{\ell=1}^{\ell_{\max}} \delta C(\ell)^2 \quad (25)$$

In particular, as we are interested in the short scale correlations, and following most of the authors in the bibliography, we adopt $\ell_{\max} = 10$.

We obtain that our nonlinearity index Δ is clearly higher during rest than during exercise (Fig. 7). For each individual subject Δ is higher for his record during rest than for his corresponding record during exercise and also the group averages are clearly different for rest and exercise ($p < 10^{-7}$). Nevertheless, we have to take into account that when dealing with relatively short records, comparisons between series of different length can lead to spurious results due to finite size effects. Here, we have that the records during exercise are two times longer than those during exercise, in addition due to the fact that HR increases with physical activity, the records during exercise are 4-5 times longer in number of beats. For this reason, we check the validity of our findings by comparing our records during rest with records of the same number of beats during exercise: consider a subject with a N_r beats record during rest and a corresponding record during exercise of length $N_e > N_r$ beats and let be $n = \lfloor N_e/N_r \rfloor$. We extract n non-overlapping windows from the exercise record starting from left to right and another n non-overlapping windows from right to left (in order to use all available data). For all these $2n$

sub-series we compute Δ and average for each subject. Results are shown in Fig. 7 (red triangles). Although now the differences between rest and exercise are a bit smaller, all the values of Δ for rest are above the corresponding values for exercise (including the error bars) and the difference between group averages is still statistically significant ($p = 3 \times 10^{-4}$).

V. CONCLUSIONS

We have obtained analytically the expression of the autocorrelation of the magnitude series $C_{|x|}$ of a linear Gaussian noise as a function of its correlation C_x as well as several analytical relations involving $C_{|x|}$, C_x and the autocorrelation of the sign series C_s . These expressions are useful to study the non-linear properties of artificial series obtained by models as well as natural series with the great advantage that our approach does not make any prior assumption about scaling or functional form of the autocorrelation functions.

In particular, we study the non-linear properties of a Gaussian model designed to produce series with multifractal properties and show that this model generates non-linear signals for all the values of the parameters even for those leading to monofractal behavior. This means that, although multifractality seems to imply non-linearity, the reverse is not always true.

We also analyze natural time series. Specifically, we have shown that the heart-beat records during rest show higher non-linearities than the records of the same subject during moderate exercise. This behavior is also achieved on average for the analyzed set of 10 semiprofessional soccer players. With this result we show that the non-linear properties of the heart-beat dynamics is yet another feature supporting that the complexity of the heart-beat is reduced during exercise. The non-linearity index proposed here has the advantage that can be evaluated on relatively small samples and does not require scaling in the autocorrelation function. It is also worth mentioning the fact that our non-linearity index is sensible to moderate exercise, this means that it could probably be applied to the study of the non-linear properties during exercise at different levels of intensity and thus, it could be of interest to study the changes in the balance between sympathetic and parasympathetic nervous systems during exercise.

VI. ACKNOWLEDGMENTS

This work is partially supported by grants: FQM-7964 and FQM-362 from the Spanish Junta de Andalucía.

Appendix A: Autocovariance of the magnitudes of two linearly correlated Gaussian variables

Consider two random variables $\{X, Y\}$, both with zero mean and unit standard deviation and following the bivariate Gaussian distribution [42]:

$$\rho(x, y) \equiv \text{Prob}\{X = x, Y = y\} = \frac{1}{2\pi\sqrt{1-K^2}} \exp\left[-\frac{x^2 + y^2 - 2Kxy}{2(1-K^2)}\right] \quad (\text{A1})$$

where $K = \langle xy \rangle$ is the covariance of variables X and Y , which also coincides with their correlation taking into account that both of them have zero mean and unit standard deviation. Note that from (A1) it follows that $K = 0$ if and only if $\{X, Y\}$ are independent, i.e. they have only linear correlations.

On the other hand, the corresponding joint probability distribution of the magnitudes can be obtained as follows:

$$\begin{aligned} F_{\text{mag}}(x, y) &\equiv \text{Prob}\{|X| \leq x, |Y| \leq y\} = \int_{-x}^x d\xi \int_{-y}^y d\varphi \rho(\xi, \varphi) \\ &= \frac{2}{\pi A_k} \int_0^x d\xi \int_0^y d\varphi \exp\left(-\frac{\xi^2 + \varphi^2}{2A_k^2}\right) \cosh\left(\frac{K\xi\varphi}{A_k^2}\right) \end{aligned} \quad (\text{A2})$$

where $A_k \equiv \sqrt{1-K^2}$, while the joint probability density of $\{|X|, |Y|\}$ is given by:

$$\rho_{\text{mag}}(x, y) = \frac{\partial^2}{\partial x \partial y} F_{\text{mag}}(x, y) = \frac{2}{\pi A_k} \exp\left(-\frac{x^2 + y^2}{2A_k^2}\right) \cosh\left(\frac{Kxy}{A_k^2}\right) \quad (\text{A3})$$

The covariance of $|X|$ and $|Y|$ is given by:

$$K_{\text{mag}} \equiv \langle |x| \cdot |y| \rangle - \langle |x| \rangle \langle |y| \rangle = \int_0^\infty x dx \int_0^\infty y dy \rho_{\text{mag}}(x, y) - \frac{2}{\pi} \quad (\text{A4})$$

where we have used that $\langle |x| \rangle = \langle |y| \rangle = \sqrt{2/\pi}$.

Now, changing the integration variables $\xi = x/A_k$ and $\varphi = y/A_k$ we obtain:

$$K_{\text{mag}} = \frac{2A_k^3}{\pi} \int_0^\infty \xi d\xi \exp\left(-\frac{\xi^2}{2}\right) \int_0^\infty \varphi d\varphi \exp\left(-\frac{\varphi^2}{2}\right) \cosh(K\xi\varphi) - \frac{2}{\pi} \quad (\text{A5})$$

The integral over φ can be written as

$$\begin{aligned} \int_0^\infty \varphi d\varphi \exp\left(-\frac{\varphi^2}{2}\right) \cosh(K\xi\varphi) &= \frac{1}{\xi} \frac{\partial}{\partial K} \left[\int_0^\infty d\varphi \exp\left(-\frac{\varphi^2}{2}\right) \sinh(K\xi\varphi) \right] \\ &= \frac{1}{\xi} \frac{\partial}{\partial K} \left[\sqrt{\frac{\pi}{2}} \exp\left(\frac{K^2\xi^2}{2}\right) \text{erf}\left(\frac{K\xi}{\sqrt{2}}\right) \right] = \sqrt{\frac{\pi}{2}} K \xi \exp\left(\frac{K^2\xi^2}{2}\right) \text{erf}\left(\frac{K\xi}{\sqrt{2}}\right) + 1, \end{aligned} \quad (\text{A6})$$

where we have used the identity [43]:

$$\int_0^\infty d\varphi e^{-b\varphi^2} \cosh(a\varphi) = \frac{1}{2} \sqrt{\frac{\pi}{b}} \exp\left(\frac{a^2}{4b}\right) \quad (\text{A7})$$

with $a = K\xi$, $b = 1/2$ and the fact that

$$\frac{d}{dx} \text{erf}(x) = \frac{2}{\sqrt{\pi}} e^{-x^2}. \quad (\text{A8})$$

Replacing (A7) in (A5)

$$K_{\text{mag}} = \sqrt{\frac{2}{\pi}} K A_k^3 \int_0^\infty \xi^2 d\xi \exp\left(-\frac{A_k^2 \xi^2}{2}\right) \text{erf}\left(\frac{K\xi}{\sqrt{2}}\right) + \frac{2A_k^3}{\pi} \int_0^\infty \xi d\xi \exp\left(-\frac{\xi^2}{2}\right) - \frac{2}{\pi} \quad (\text{A9})$$

and using the identity [44]

$$\begin{aligned} \int_0^\infty \xi^2 d\xi \exp(-b^2 \xi^2) \text{erf}(a\xi) &= \frac{\sqrt{\pi}}{4b^3} \text{sign}(a) - \frac{1}{2\sqrt{\pi}} \left[\frac{1}{b^3} \arctan\left(\frac{b}{a}\right) - \frac{a}{b^2(a^2 + b^2)} \right] \\ \text{with } a &= \frac{K}{\sqrt{2}}, b = \frac{A_k}{\sqrt{2}} \end{aligned} \quad (\text{A10})$$

$$\begin{aligned}
K_{\text{mag}} &= |K| + \frac{2}{\pi} \left[K^2 A_k + A_k^3 - K \arctan \left(\frac{A_k}{K} \right) - 1 \right] \\
&= |K| + \frac{2}{\pi} \left[\sqrt{1 - K^2} - K \arctan \left(\frac{\sqrt{1 - K^2}}{K} \right) - 1 \right],
\end{aligned} \tag{A11}$$

Finally, after some trigonometric manipulation:

$$K_{\text{mag}} = \frac{2}{\pi} \left(\sqrt{1 - K^2} + K \arcsin K - 1 \right). \tag{A12}$$

Appendix B: Autocovariance of the squares of two linearly correlated Gaussian variables

Considering again, as in Appendix A, two Gaussian variables $\{X, Y\}$ following the bivariate Gaussian distribution (A1), the autocovariance of their squares is given by:

$$\begin{aligned}
K_{\text{sq}} &= \langle x^2 \cdot y^2 \rangle - \langle x^2 \rangle \langle y^2 \rangle = \int_{-\infty}^{\infty} x^2 dx \int_{-\infty}^{\infty} y^2 dy \rho(x, y) - 1 \\
&= \frac{1}{2\pi A_k} \int_{-\infty}^{\infty} x^2 \exp \left(-\frac{x^2}{2A_k^2} \right) \int_{-\infty}^{\infty} y^2 \exp \left(-\frac{y^2}{2A_k^2} \right) \exp \left(-\frac{Kxy}{A_k^2} \right) - 1,
\end{aligned} \tag{B1}$$

where we have used that $\langle x^2 \rangle = \langle y^2 \rangle = 1$. Now, changing the integration variables $\xi = x/A_k$ and $\varphi = y/A_k$ we obtain:

$$\begin{aligned}
K_{\text{sq}} &= \frac{A_k^5}{2\pi} \int_{-\infty}^{\infty} \xi^2 d\xi \exp \left(-\frac{\xi^2}{2} \right) \underbrace{\int_{-\infty}^{\infty} \varphi^2 d\varphi \exp \left(-\frac{\varphi^2}{2} \right) \exp(-K\varphi\xi)}_{\sqrt{2\pi} e^{\frac{K^2 \xi^2}{2}} (1 + K^2 \xi^2)} - 1
\end{aligned} \tag{B2}$$

taking into account that $A_k^2 = 1 - K^2$:

$$\begin{aligned}
K_{\text{sq}} &= \frac{A_k^5}{\sqrt{2\pi}} \left[\int_{-\infty}^{\infty} \xi^2 d\xi e^{-\frac{A_k^2 \xi^2}{2}} + K^2 \int_{-\infty}^{\infty} \xi^4 d\xi e^{-\frac{A_k^2 \xi^2}{2}} \right] - 1 \\
&= \frac{A_k^2}{\sqrt{2\pi}} \int_{-\infty}^{\infty} x^2 dx e^{-\frac{x^2}{2}} + \frac{K^2}{\sqrt{2\pi}} \int_{-\infty}^{\infty} x^4 dx e^{-\frac{x^2}{2}} - 1,
\end{aligned} \tag{B3}$$

and finally:

$$K_{\text{sq}} = 2K^2 \tag{B4}$$

[1] C. K. Peng et al.: Long-range anticorrelations and non-Gaussian behavior of the heartbeat. *Phys. Rev. Lett.* **70**, 1343 (1993).

[2] Nature (1996).

[3] A. L. Goldberger, et al.: Fractal dynamics in physiology: Alterations with disease and aging. *Proc. Natl. Acad. Sci. USA* **99**, 2466-2472 (2002).

[4] P. Ch. Ivanov, et al.: Sleep-wake differences in scaling behavior of the human heartbeat: Analysis of terrestrial and long-term space flight data. *Europhys. Lett.* **48**(5), 594-600 (1999).

[5] A.E. Aubert, B. Seps and F. Beckers: Heart Rate Variability in Athletes. *Sports Med.* **33**(12), 889-919 (2003).

[6] J.G. Dong: The role of heart rate variability in sports physiology (Review). *Experimental and Therapeutic Medicine* **11**, 1531-1536 (2016).

[7] R. T. Baillie, A. A. Cecen and C. Erakl: Normal heartbeat series are nonchaotic, nonlinear, and multifractal: New evidence from semiparametric and parametric tests. *Chaos* **19**, 028503 (2009).

[8] P. Ch. Ivanov, et al.: Multifractality in human heartbeat dynamics. *Nature* **399**(6735), 461-465 (1999).

[9] Y. Ashkenazy, et al.: Magnitude and Sign Correlations in Heartbeat Fluctuations. *Phys. Rev. Lett.* **86**, 1900-1903 (2001).

[10] Y. Ashkenazy, et al.: Nonlinearity and multifractality of climate change in the past 420,000 years. *Geophys. Res. Lett.* **30**(22), 2146 (2003).

[11] T. Schreiber & A. Schmitz: Surrogate time series. *Physica D* **142**, 346382 (2000).

[12] P. Allegrini, M. Barbi, P. Grigolini, B. J. West: Dynamical model for DNA sequences, *Phys. Rev. E* **52**, 5281 (1995).

[13] G. Rangarajan & M. Ding: Integrated approach to the assessment of long range correlation in time series data. *Phys. Rev. E* **61**, 4991 (2000).

[14] L. Zhu et al.: Magnitude and sign correlations in conductance fluctuations of horizontal oil water two-phase flow. *J. Phys. Conf. Ser.* **364**, 012067 (2012).

[15] I. Bartos and I.M. Jánosi: Nonlinear correlations of daily temperature records over land. *Nonlin. Processes Geophys.* **13**, 571-576 (2006).

[16] Q. Li, Z. Fu, N. Yuan and F. Xie: Effects of non-stationarity on the magnitude and sign scaling in the multi-scale vertical velocity increment. *Physica A* **410**, 9-16 (2014).

[17] Y.H. Liu, et al.: Statistical properties of the volatility of price fluctuations. *Phys. Rev. E* **60**, 1390-1400 (1999).

[18] T. Kalisky, Y. Ashkenazy and S. Havlin: Volatility of linear and nonlinear time series. *Phys. Rev. E* **72**, 011913 (2005).

[19] M. Gómez-Extremera, P. Carpena, P.Ch. Ivanov and P.A. Bernaola-Galván: Magnitude and sign of long-range correlated time series: Decomposition and surrogate signal generation. *Phys. Rev. E* **93**, 042201 (2016).

[20] M. A. Peña, J. C. Echeverría, M.T. García and R. González-Camarena: Applying fractal analysis to short sets of heart rate variability data. *Med. Biol. Eng. Comput.* (2009) **47**, 709-717 (2009).

[21] M. Höll & H. Kantz: The fluctuation function of the detrended fluctuation analysis investigation on the AR(1) process. *Eur. Phys. J. B* **88**, 126 (2015).

[22] P. Perikakis, et al.: Breathing frequency bias in fractal analysis of heart rate variability. *Biological Psychology* **82**, 82-88 (2009).

[23] G.R.H. Sandercock & D.A. Brodie: The use of heart rate variability measures to assess autonomic control during exercise. *Scand. J. Med. Sci. Sports* **16** 302-313 (2006).

[24] P. Carpena, M. Gómez-Extremera, C. Carretero-Campos, P. Bernaola-Galván and A.V. Coronado: Spurious results of Fluctuation Analysis techniques in magnitude and sign correlations. Submitted to *Entropy* (2017).

[25] J.W Kantelhardt et al. Multifractal detrended fluctuation analysis of nonstationary time series. *Physica A* **316**, 87 (2002).

[26] H. A. Makse, S. Havlin, M. Schwartz and H. E. Stanley: Method for generating long-range correlations for large systems. *Phys. Rev. E* **53**, 5445 (1996).

[27] J. Beran, *Statistics for Log-memory Processes* (Chapman & Hall, New York, 1994).

[28] C.-K. Peng, S.V. Buldyrev, S. Havlin, M. Simons, H.E. Stanley, and A.L. Goldberger: Mosaic organization of DNA nucleotides. *Phys. Rev. E* **49**, 1685-1689 (1994).

[29] C. Carretero-Campos, P. Bernaola-Galván, P. Ch. Ivanov and P. Carpena: Phase transitions in the first-passage time of scale-invariant correlated processes. *Phys. Rev. E* **85**, 011130 (2012).

[30] S. S. Apostolov, F. M. Izrailev, N. M. Makarov, Z. A. Mayzelis, S. S. Melnyk, O. V. Usatenko: The Signum function method for the generation of correlated dichotomic chains. *J. Phys. A: Math. Theor.* **41**, 17501 (2008).

[31] G. Parisi & U. Frisch: On the singularity structure of fully-developed turbulence, in *Turbulence and predictability in geophysical fluid dynamics*, Proc. Int. School E. Fermi, edited by M. Ghil et al., North Holland (1985).

[32] G. Badin & D. I. V. Domeisen: Nonlinear stratospheric variability: multifractal de-trended fluctuation analysis and singularity spectra. *Proc. R. Soc. A.* **472**: 20150864 (2016).

[33] L. Tang, et al.: Complexity testing techniques for time series data: A comprehensive literature review. *Chaos, Solitons & Fractals* **81**, 117 (2015).

[34] S. Sarmiento et al.: Heart rate variability during high-intensity exercise. *J Syst Sci Complex* **26** 104-116 (2013).

[35] O. Anosov, A. Patzak and Y. Kononovich: High-frequency oscillations of the heart rate during ramp load reflect the human anaerobic threshold. *Eur. J. Appl. Physiol* **83**, 388-394 (2000).

[36] M. J. Lewis & A. L. Short: Exercise and cardiac regulation: what can electrocardiographic time series tell us? *Scand. J. Med. Sci. Sports* **20** 794-804 (2010).

[37] M.M. Platisa et al.: Complexity of heartbeat interval series in young healthy trained and untrained men. *Physiol. Meas.* **29**, 439-450 (2008).

[38] R. Karasik et al.: Correlation differences in heartbeat fluctuations during rest and exercise. *Phys Rev. E* **66**, 062902 (2002).

[39] A.J. Hautala et al.: Short-term correlation properties of R-R interval dynamics at different exercise intensity levels. *Clin Physiol. Funct. Imagin* **23**, 215-223 (2003).

[40] M. P. Tulppo et al.: Effects of exercise and passive head-up tilt on fractal and complexity properties of heart rate dynamics. *Am J. Physiol. Heart Circ. Physiol.* **280**, H1081-H1087 (2001).

[41] M. Weippert, et al.: Comparison of three mobile devices for measuring R-R intervals and heart rate variability: Polar S810i, Suunto t6 and an ambulatory ECG system. *European Journal of Applied Physiology* **109**(4), 779-786 (2010).

[42] R. A. Johnson & D.W. Wichern: *Applied Multivariate Statistical Analysis*. (6th Ed. Pearson Prentice Hall, New Jersey 2007).

[43] I.S.Gradshteyn & I.M. Ryzhik: *Table of Integrals, Series and Products*. (Academic Press, New York 1980). Page 356.

[44] E.W. Ng & M. Geller: A Table of Integrals of the Error Functions. *J. Res. Nat. Bur. Standards Sect. B* **73B**, 1-20 (1969).